

Duquesne Light Company

Beaver Valley Power Station
P.O. Box 4
Shippingport, PA 15077-0004

SUSHIL C. JAIN
Division Vice President
Nuclear Services
Nuclear Power Division

(412) 393-5512
Fax (412) 643-8069

April 23, 1996

U. S. Nuclear Regulatory Commission
Attention: Document Control Desk
Washington, DC 20555-0001

**Subject: Beaver Valley Power Station, Unit No. 1
Docket No. 50-334, License No. DPR-66
Analysis of Flaw Indications:
1989 Edition of ASME XI, Article IWB-3640**

The purpose of this letter is to submit, for NRC review and approval, an analytical evaluation of an indication identified during non-destructive examinations (NDE) of Class 1 austenitic piping that exceeds the acceptance criteria specified in Section XI of the ASME Boiler and Pressure Vessel (B&PV) Code. NRC approval is requested at this time to support the return to service of Unit No. 1 from the current eleventh refueling outage. It is requested that the review of the analytical evaluation be completed in time to support the transition to Mode 4 presently scheduled for May 4, 1996. This request is being pursued as a contingency effort to provide the NRC sufficient review time. For the purpose of returning Unit 1 to power, the Duquesne Light Co. is conservatively considering this a flaw indication as it continues indication characterization evaluation. Additionally, as a conservative measure to minimize the impact on the present outage duration, the examination scope has been expanded in accordance with Article IWB-2430.

Unit No. 1 is currently in its eleventh refueling outage and in the third period of the second ten-year inservice inspection interval. While conducting volumetric NDEs on reactor coolant system (RCS) "C" loop cold leg pressure retaining piping weld number DLW-LOOP3-7-S-02, an indication was identified which exceeded the Code acceptance criteria in Table IWB-3514-2. The Beaver Valley applicable ASME B&PV Code, Section XI, is the 1983 Edition through Summer 1983 Addenda.

Article IWB-3122.4 provides for inservice NDE acceptance by evaluation as described in IWB-3600; however, this Article applies to ferritic steel components or steam generator tubing and does not provide an analytical method for evaluating indications in austenitic stainless steel.



300095

9604300327 960423
PDR ADOCK 05000334
Q PDR

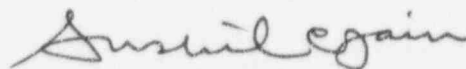
A027
411

The 1989 Edition of ASME Section XI is the most recent edition approved by the NRC and referenced for use in 10 CFR 50.55a(b)(2). Article IWB-3640 of that edition provides evaluation procedures and acceptance criteria for austenitic piping and includes reference to Appendix C for the analytical procedures for flaw evaluation. The enclosed Westinghouse letter report summarizes the bounding analysis, based on elastic-plastic fracture mechanics. This analysis demonstrates that the assumed flaw indication in the RCS "C" loop cold leg is acceptable for continued service until the end of service lifetime. Unless characterized as a reflector, future inspections will be conducted as required by ASME Section XI Article IWB-2420. This requires reexamination of this weld during the next three inspection periods. As such, this weld will be examined once during each of the next three 40-month periods.

Additional examinations of the identified indication are being done in parallel with this bounding analysis in an attempt to determine if the indication can be resolved in accordance with IWB-3514.5, Ultrasonic Reflectors of Geometric and Metallurgical Origin. This article provides the methodology to characterize the indication as a reflector, and not an indication, due to surface configuration or variations in metallurgical structure of materials at interfaces. These additional examinations and a complete review of the fabrication records are in progress to assist in the final disposition of the subject indication. A follow-up to this letter will be submitted by May 1, 1996, docketing the Duquesne Light Company weld disposition.

If you have any questions regarding this request, please contact Mr. Roy K. Brosi at (412) 393-5210.

Sincerely,



Sushil C. Jain

Enclosure

c: Mr. L. W. Rossbach, Sr. Resident Inspector
Mr. T. T. Martin, NRC Region I Administrator
Mr. D. S. Brinkman, Sr. Project Manager

Evaluation of Indications in the Beaver Valley Unit 1 Cold Leg Piping to 40 Degree Elbow Weld Region

During the recent 20 year plant in-service inspection at Beaver Valley Unit 1, ultrasonic examination of the reactor coolant loop piping revealed an indication at the cold leg loop pipe to elbow weld of loop "C". This examination was done in accordance with ASME Section XI, 1983 Edition with the Summer 83 Addenda. At the request of Duquesne Light Company an assessment of the indication was performed to determine whether this indication would remain within ASME Section XI Appendix C evaluation acceptance standards. The evaluation has been performed in accordance with the criteria of IWB 3640 of ASME Section XI, 1989 Edition, since no evaluation guidance is given in the 1983 Edition for indications in austenitic materials.

1.0 NDE EVALUATION

1.1 Weld Fabrication Information

Weld DLW-LOOP3-7-S-02 is a 27-1/2" ID circumferential butt weld joining a 35°-23'-26" static cast A351 Grade CF8M elbow to A351 Grade A351 CF8M centrifugally cast pipe. The weld is a shop weld fabricated by SouthWest Fabricating and Welding in 1971.

Weld Filler material is TP 308 stainless steel. The weld was made using a TIG weld process for the root passes. It is believed that the remaining weld passes were made using a submerged arc welding process based on the weld appearance and observation of other circumferential welds on the sister train spool pieces which were radiographed in the as-welded condition. (A review of the fabrication records confirmed the use of a tig root pass with the balance of the weld being done by the sub-merged ARC process.)

The weld is the first circumferential weld after the Reactor Vessel nozzle-to-safe-end weld on the C loop cold leg (the other end of the elbow is welded to the RV safe-end). The geometry is shown in Figure 1.

1.2 UT Instrumentation and Sensitivity Comparisons

Initial UT examination (Report UT96-4) was conducted on 3/26/96 using a 45 degree dual element refracted longitudinal search unit set. (KFA Alpha series 1.0 Mhz., 1.0" diameter). The UT instrument used was a Panametrics Epoch with modified bandpass filter. This combination has been demonstrated to be effective in examining centrifugally cast stainless steel pipe. A second examination (Report UT96-5) was conducted on 3/27/96 to verify the indication and allow the Duquesne Light Company and vendor Level III UT examiners to observe the indication. This examination used the same instrumentation.

A third UT examination was conducted on 3/29/96 using a Panametrics Epoch II instrument with a newly developed KBA ceramic composite search unit provided by Wesdyne. This search unit uses 30x40mm dual elements in an integral case providing a 37 degree refracted longitudinal wave. The primary purpose of this scan was to confirm the reflector using another angle and try to observe any additional signal dynamics or tip diffracted peaks that may be generated. In addition, the 45 degree search units were once again used to observe

the response using this instrument. Instrument screen signal peak and forward-backward points were also digitized to include in this report to illustrate actual screen signal images.

The UT examinations conducted during the first 10 year interval used calibration block BV1-1 for sensitivity. This block did not meet the requirements for the current Code and is no longer used. Examinations on cast stainless piping welds during this interval used block PP-2, which is the Unit 2 RCS calibration block. A comparison was conducted for axial direction calibration sensitivity and showed that the currently used PP-2 block is 7 dB more sensitive than the older BV1-1 block. This means that the 200% DAC indication observed would have been nearly 100% DAC using an examination sensitivity based on BV1-1.

1.3 Previous Ultrasonic Examinations

The weld was examined initially in 3/75 by Westinghouse (no indications) and again in 5/86 by B&W (No recordable indications for either circumferential or axial examinations).

Fabrication radiographs were recalled and reviewed on 3/28/96. This review revealed no root irregularities that should cause the signals observed.

1.4 UT Signal Characteristics and Evaluation

The examination conducted on 3/29/96 (Report UT-96-6) revealed the following information:

Indication 800 (37° RL from side 1) was 200% DAC, peak response at 12" from TDC, extending from 9" to 13.5" from TDC (4.5 inches long).

Indication 801 (37° R/L from side 2) was 100% DAC, peak response at 8" from TDC, extending from 4" to 10.5" from TDC (6.5" long).

Indication 200 (45° R/L from side 1) was 159% DAC, peak response at 12.75" from TDC, extending from 9" to 14" from TDC (5" long).

Indication 201 (45° R/L from side 2) was 100% DAC, peak response at 12.5" from TDC, extending from 8" to 14" from TDC (6" long).

The lengths observed are longer than initially reported. Initial examination procedure instructions limit length to the point where the signal drops to 50% of its maximum amplitude. The dimensions reported show lengths where the signal drops to baseline noise.

A follow-up examination was conducted on the inside surface of the pipe using a driver pickup eddy current probe. The probe was set such that the coil labeled "in-line" was oriented to be sensitive to circumferentially oriented notches in a cast stainless steel calibration block. The outputs available from the eddy current instrument are a video output, vertical component of lissajous signal and a horizontal component of lissajous signal. The video output was recorded on a high resolution video recording tape. This served as a primary data of record for analysis. The horizontal and vertical components were conditioned using a bias amplifier, synchronized with the tool encoders and digitized using the UDRPS. This digitized data provided C-scans which enabled us to get a good overall feel for the quality of data.

The eddy current probe was used to do a complete surface examination of the elbow to pipe weld region of the cold leg for all three loops. The results of these circumferential scans were essentially identical for all three loops, and showed no surface breaking indications. Even though this examination confirmed the lack of any surface indications, the fracture mechanics analysis used an umbrella of all the UT characterized indications, for conservatism, assuming the indication to be surface breaking.

The indication which was evaluated is a single composite size which bounds all four of these indications. It extends circumferentially from the four inch position to the 14 inch position, and has the following dimensions:

a = 0.68 inches
ℓ = 10 inches
t = 2.66
a/t = 25.6%
a/ℓ = 0.07

2.0 FRACTURE ANALYSIS METHODS AND MATERIAL PROPERTIES

2.1 Fracture Toughness

The inlet elbow is cast stainless steel SA351, type CF8M. The pipe to elbow weld was made by submerged arc process, with a root pass TIG weld.

The fracture toughness of the base metal and TIG weld has been found to be very high, even at operating temperatures [2], where the J_{Ic} values have been found to be well over 2000 in lb/in². Fracture toughness values for flux weld materials have been found to display much more scatter, with the lowest reported values significantly lower than the base metal toughness. Although the J_{Ic} values reported have been lower, the slope of the J-R-curve is still large for these lower J_{Ic} cases. Representative values for J_{Ic} were obtained from the results of Landes and co-workers [3], where the following value was obtained, and was used in the development of the fracture evaluation methods.

for submerged arc welds: $J_{Ic} = 650$ in lb/in².

It should be mentioned here that the above properties are bounding for all weld types.

2.2 Allowable Flaw Size Determination

The critical flaw size is not directly calculated as part of the flaw evaluation process for stainless steels. Instead, the failure mode and critical flaw size are incorporated directly into the flaw evaluation technical basis, and therefore into the tables of "Allowable End-of-Evaluation Period Flaw Depth to Thickness Ratio," which are contained in paragraph IWB 3640. A more accurate determination of the allowable depth can be made using the methodology of Appendix C, and this was the approach used here.

Rapid, nonductile failure is possible for ferritic materials at low temperatures, but is not applicable to stainless steels. In stainless steel materials, the higher ductility leads to two possible modes of failure, plastic collapse or unstable ductile tearing. The second mechanism can occur when the applied J integral exceeds the J_{Ic} fracture toughness, and some stable tearing occurs prior to failure. If this mode of failure is dominant, the load carrying capacity is less than that predicted by the plastic collapse mechanism.

The allowable flaw sizes of paragraph IWB 3640 for the high toughness base materials were determined based on the assumption that plastic collapse would be achieved and would be the dominant mode of failure. However, due to the reduced toughness of the submerged arc and shielded metal arc welds, it is possible that crack extension and unstable ductile tearing could occur and be the dominant mode of failure. This consideration in effect reduces the allowable end of interval flaw sizes for flux welds relative to the austenitic wrought piping, and has been incorporated directly into the evaluation. The pipe design loads are listed in Table 1, and the most governing loads for each category were used in the evaluation.

2.3 Stress Corrosion Cracking Susceptibility

In evaluating flaws, all mechanisms of subcritical crack growth must be evaluated to ensure that proper safety margins are maintained during service. Stress corrosion cracking has been observed to occur in stainless steel in operating BWR piping systems; the discussion presented here is the technical basis for not considering this mechanism in the present analysis.

For all Westinghouse plants, there is no history of cracking failure in the reactor coolant system loop piping. For stress corrosion cracking (SCC) to occur in piping, the following three conditions must exist simultaneously: high tensile stresses, a susceptible material, and a corrosive environment. Since some residual stresses and some degree of material susceptibility exist in any stainless steel piping, the potential for stress corrosion is minimized by proper material selection immune to SCC as well as preventing the occurrence of a corrosive environment. The material specifications consider compatibility with the system's operating environment (both internal and external) as well as other materials in the system, applicable ASME Code rules, fracture toughness, welding, fabrication, and processing.

The environments known to increase the susceptibility of austenitic stainless steel to stress corrosion are oxygen, fluorides, chlorides, hydroxides, hydrogen peroxide, and reduced forms of sulfur (e.g., sulfides, sulfites, and thionates). Strict pipe cleaning standards prior to operation and careful control of water chemistry during plant operation are used to prevent the occurrence of a corrosive environment. Prior to being put into service, the piping is cleaned internally and externally. During flushes and preoperational testing, water chemistry is controlled in accordance with written specifications. External cleaning for Class 1 stainless steel piping includes patch tests to monitor and control chloride and fluoride levels. For preoperational flushes, influent water chemistry is controlled. Requirements on chlorides, fluorides, conductivity, and pH are included in the acceptance criteria for the piping.

During plant operation, the reactor coolant system (RCS) water chemistry is monitored and maintained within very specific limits. Contaminant concentrations are kept below the thresholds known to be conducive to stress corrosion cracking with the major water chemistry control standards being included in the plant operating procedures as a condition for plant operation. For example, during normal power operation, oxygen concentration in the RCS is expected to be less than 0.005 ppm by controlling charging flow chemistry and maintaining hydrogen in the reactor coolant at specified concentrations. Halogen concentrations are also stringently controlled by maintaining concentrations of chlorides and fluorides within the specified limits. This is assured by controlling charging flow chemistry and specifying proper wetted surface materials.

2.4 Thermal Aging

Thermal aging at operating temperatures of reactor primary piping can reduce the fracture toughness of cast stainless steels and, to a lesser degree, stainless steel weldments. The cast stainless steel piping and elbows of the primary loop are very tough, usually exhibiting J_{Ic} values exceeding 2000 in-lb/in² and a tearing modulus, T_{mat} , well over 200. NRC procedures exist for addressing the impact of thermal aging on fracture toughness for full-service life. The approved procedures were applied to the inlet elbow containing the indication. The elbow

was fabricated of CF8M cast stainless steel, which is the same material as the pipe to which it is welded. It was found that the elbow qualified for the highest assignable end-of-service fracture toughness values by the NRC-approved procedure, specifically, $J_{Ic} = 750 \text{ in-lb/in}^2$, $T_{mat} = 60$.

On the other side of the weld is a straight pipe which has a relatively high ferrite content (15.7%) and which does not qualify for the highest fracture toughness values after thermal aging. The aging assessment for Loop 3 where the indication is located results in an aging parameter of 2.36, which is just below the threshold value of 2.4 needed to justify the higher toughness. The fully aged toughness of this pipe material was estimated to be $J_{Ic} = 410 \text{ in-lb/in}^2$, so this value was used as the governing value of toughness after thermal aging[9].

Even with thermal aging, equivalent to full service for SAW welds, the tearing modulus remains high (>100) and the unaged toughness, J_{Ic} , is not significantly reduced. Therefore the value of $J_{Ic} = 650 \text{ in-lb/in}^2$ from ASME Code Section XI was retained for this analysis. Because of the larger tearing modulus, SAW welds with full service life aging remain as good as the elbow material in question from a stability view point.

Thus, the fracture toughness values applicable for full service life are

$J_{Ic} = 750 \text{ in-lb/in}^2$, $T_{mat} = 60$ for the elbow, $J_{Ic} = 650 \text{ in-lb/in}^2$
and $T_{mat} = 100$ for the SAW weld and $J_{Ic} = 410 \text{ in-lb/in}^2$ and $T_{mat} = 13$ for the piping. It should be recognized that these values are believed to be very conservative estimates of the end of life fracture properties.

The limiting properties are those of the piping, and these properties were used in construction of the flaw evaluation charts.

3.0 FATIGUE CRACK GROWTH

In applying the ASME Code Section XI Code acceptance criteria, the final flaw size a_f used in the criteria is defined as the flaw size to which the detected flaw is calculated to grow at the end of the design life, or until the next inspection time.

To determine the fatigue crack growth in the elbow to pipe weld region, an analysis was carried out for the actual location of interest. The loadings used included thermal and deadweight piping loads, pressure and thermal transient loads, and residual stresses. Thermal aging has been shown not to impact fatigue crack growth, so the reference crack growth curve was not changed, as discussed further in Section 3.1.

3.1 Analysis Methodology

The analysis procedure involves postulating an initial flaw at each specific region and predicting the growth of that flaw due to an imposed series of loading transients. The input required for a fatigue crack growth analysis is basically the information necessary to calculate the parameter ΔK_I (range of stress intensity factor) which depends on crack and structure geometry and the range of applied stresses in the area where the crack exists. Once ΔK_I is calculated, the growth due to that particular stress cycle can be calculated by equations given in section 3.4. This increment of growth is then added to the original crack size, and the analysis proceeds to the next transient. The procedure is continued in this manner until all the transients known to occur in the period of evaluation have been analyzed.

The transients considered in the analysis are all the design transients contained in the equipment specification, as shown in Table 2. It should be noted that the Beaver Valley plants were designed to a slightly different set of transients than those used in the analysis here. Although the design transients are not identical, they are very similar. The transients used are the most up-to-date set available. In general, the transients used in these analyses are more numerous than those for Beaver Valley. The transients which have been used as the design basis for later plants are generally more accurate, because they reflect greater operating experience. For this reason the transients used in the evaluation charts are considered to be conservative, relative to the original design transients.

These transients are spread equally over the design lifetime of the plant, with the exception that the preoperational tests are considered first. Faulted conditions are not considered because their frequency of occurrence is too low to affect fatigue crack growth.

3.2 Residual Stresses

Since the piping weld of interest here was not stress-relieved, residual stresses are clearly present. For fatigue crack growth analyses, these stresses were included directly, using as a guide the residual stress values in the technical basis document for the ASME Code flaw evaluation procedures [4].

Although there is significant residual stress variation from one weldment to another, there have been a large number of measurements made, and these were collected in reference [4]. These stresses were used directly in the analysis, except in a few instances where the

elastically calculated stresses were significantly above yield stress. In these cases it would be unrealistic to add the residual stresses, so they were not used. It should be noted here that the residual stresses were added to both the maximum and minimum stresses, and therefore do not affect the stress range. Their effect is seen only through the R ratio.

3.3 Stress Intensity Factor Expressions

Stress intensity factors were calculated from methods available in the literature for each of the flaw types analyzed. The surface flaw with aspect ratio 6:1 is analyzed using an expression developed by McGowan and Raymond [5] where the stress intensity factor K_I is calculated from the actual stress profile through the wall at the location of interest.

The maximum and minimum stress profiles corresponding to each transient are represented by a third order polynomial such that:

$$\sigma(x) = A_0 + A_1 \frac{x}{t} + A_2 \frac{x^2}{t^2} + A_3 \frac{x^3}{t^3}$$

The stress intensity factor $K_I(\phi)$ can be calculated anywhere along the crack front. The point of maximum crack depth is represented by $\phi = 0$. The following expression is used for calculating $K_I(\phi)$.

$$K_I(\phi) = \left(\frac{\pi a}{Q}\right)^{0.5} (\cos^2 \phi + \frac{a^2}{c^2} \sin^2 \phi)^{1/4} (A_0 H_0 + \frac{2a}{\pi t} A_1 H_1 + \frac{1}{2} \frac{a^2}{t^2} A_2 H_2 + \frac{4}{3} \pi \frac{a^3}{t^3} A_3 H_3)$$

The magnification factors H_0 , H_1 , H_2 and H_3 are a function of d and are obtained by the procedure outlined in reference [5].

The stress intensity factor for a continuous surface flaw was calculated using an expression for an edge cracked plate [6]. The stress distribution is linearized through the wall thickness to determine the membrane and bending stresses; the applied K_I is calculated from:

$$K_I = \sigma_m Y_m (\pi a)^{0.5} + \sigma_B Y_B (a\pi)^{0.5}$$

The magnification factors Y_m and Y_B are taken from [6] and "a" is the crack depth.

3.4 Crack Growth Rate Reference Curves

There is presently no reference fatigue crack growth rate curve in the ASME Code for austenitic stainless steels in a PWR water environment. However, a great deal of work has been done recently which supports the development of such a curve. An extensive study was done by the Metals Property Council working group on reference fatigue crack growth concerning the crack growth behavior of these steels in air environments, published in reference [7]. A reference curve for stainless steels in air environments, based on this work, was published in the 1988 Addenda of Section XI.

A compilation of data for austenitic stainless steels in a PWR water environment was made by Bamford [8], and it was found that the effect of the environment on the crack growth rate was very small. From this information it was estimated that the environmental factor should be conservatively set at 2.0 in the crack growth rate equation from reference [7]. Therefore the crack growth rate equation used in the analysis was:

$$\frac{da}{dn} = C F S E \Delta K^{3.30}$$

where:

- C = 2.42×10^{-20}
- F = frequency factor (F = 1.0 for temperatures below 800°F)
- S = R ratio correction (S = 1.0 for R = 0; S = 1 + 1.8R for 0 < R < .8; and S = -43.35 + 57.97R for R > 0.8)
- E = environmental factor (E = 2.0 for PWR environment)
- ΔK = range of stress intensity factor, in psi $\sqrt{\text{in}}$

and R is the ratio of the minimum K_I to the maximum K_I .

3.5 Fatigue Crack Growth Results

The results of the crack growth analysis work are shown in Table 3. Table 3 shows results for circumferential surface flaws of several different aspect ratios. The top entry of the table is for an indication extending entirely around or along the pipe, while the entries below are for indications with various aspect ratios. It is clear from this table that the crack growth predicted during future service is not significant.

4.0 RESULTS

4.1 Construction of the Surface Flaw Evaluation Chart

Two basic dimensionless parameters can fully address the characteristics of a surface flaw, and are used for the evaluation chart construction:

- Flaw Shape Parameter a/ℓ
- Flaw Depth Parameter a/t

where:

- t = wall thickness, in.
- a = flaw depth, in.
- ℓ = flaw length, in.

A typical chart was chosen for illustration purpose as follows: (Refer to Figure 2)

- The flaw shape parameter a/ℓ was plotted as the abscissa from 0 (continuous flaw) to .5
- The flaw depth parameter a/t in % was plotted as the ordinate.
- The lower curve is the Code acceptable flaw depth tabulated in Table IWB-3514-2 of ASME Section XI. This curve indicates the acceptance standards of the Code, below which analytical evaluation is not required.
- The upper boundary curve shows the maximum acceptable flaw depth beyond which no surface flaw is acceptable for continued service without repair. This upper bound curve has been determined by the fracture and fatigue evaluations described herein.
- Any surface indication which falls between the two boundary curves will be acceptable by the Code, with the analytical justification provided herein. However, IWB-2420 of ASME Section XI requires future monitoring of such indications.

Step 1

Determine the allowable flaw depths for a range of flaw shapes. These flaw sizes were determined directly from the equations of Appendix C.

Load Condition	Flaw Orientation	Allowable Flaw Depth (in.)			
		$a/l = 0.001$	$a/l = 0.025$	$a/l = 0.05$	$a/l = 0.1$
N/U/T*	Circumferential	$a/t = 0.453$	$a/t = 0.476$	$a/t = 0.610$	$a/t = 0.831$
E/F*	Circumferential	$a/t = 0.365$	$a/t = 0.407$	$a/t = 0.536$	$a/t = 0.736$

* N/U/T normal, upset, and test conditions
E/F emergency and faulted conditions

The allowable flaw depth for the emergency and faulted conditions is more limiting.

Step 2

Determine the corresponding initial flaw sizes which will grow to the above allowable flaw sizes after 10, 20, and 30 years of service. We define the above limiting allowable flaw depth as a_r . The initial flaw size a_o can be found from the fatigue crack growth results. The values of a_o which are applicable to 10 years of service, for example, are listed as follows:

	$a/l = 0.01$	$a/l = 0.025$	$a/l = 0.05$	$a/l = 0.1$
a_{in}	0.365	0.407	0.536	0.60
a_{o1}	0.361	0.402	0.531	0.597

This shows that the effect of fatigue crack growth in this region is relatively small.

Step 3

The upper bound curves result from the plots of a/l vs. a/t for 10, 20, 30 years of service, as obtained from the crack growth results. These curves are shown in Figure 2.

Step 4

Plot a/l vs. a/t data from the standards tables of Section XI as the lower curve of Figure 2.

The values of Table IWB-3514-2 of Section XI for a pipe wall thickness of 2.66 inches are:

Aspect Ratio, a/l	Surface Indication, $a/t, \%$
0.00	9.75
0.05	9.9
0.1	10.1
0.15	10.2

Aspect Ratio, <u>a/l</u>	Surface Indication, <u>a/t, %</u>
0.20	10.4
0.25	10.6
0.30	10.8
0.35	10.9
0.40	11.1
0.45	11.3
0.50	11.4

The above four steps complete the procedure for the construction of the surface flaw evaluation charts for 10 years, 20 years, or 30 years of operating life.

4.2 Flaw Evaluation Results

The flaw evaluation is completed by simply plotting the maximum indication size as summarized in Section 1.4 on the flaw evaluation chart of Figure 2. The result is that the indication is acceptable for further service without repair.

It can be seen from Figure 2 that the indication is acceptable with a large margin, even though a maximum bounding indication size has been used. The large margin shown here should eliminate any concerns about the accuracy of the inspection, since the flaw could be significantly larger, and still be acceptable.

5.0 REFERENCES

1. ASME Code Section XI, "Rules of Inservice Inspection of Nuclear Power Plant Components," 1983 edition (used for updated code allowable limits); 1986 edition (used for stainless steel flaw evaluation).
2. Bamford, W. H. and Bush, A. J., "Fracture of Stainless Steel," in Elastic Plastic Fracture, ASTM STP 668, 1979.
3. Landes, J. D., and Norris, D. M., "Fracture Toughness of Stainless Steel Piping Weldments," presented at ASME Pressure Vessel Conference, 1984.
4. "Evaluation of Flaws in Austenitic Steel Piping," Trans ASME, Journal of Pressure Vessel Technology, Vol. 108, Aug. 1986, pp. 352-366.
5. McGowan, J. J. and Raymond, M., "Stress Intensity Factor Solutions for Internal Longitudinal Semi-elliptic Surface Flaw in a Cylinder Under Arbitrary Loading," ASTM STP 677, 1979, pp. 365-380.
6. Plane Strain Crack Toughness Testing of High Strength Metallic Materials, ASTM STP 410, March 1969.
7. James, L. A., and Jones, D. P., "Fatigue Crack growth Correlations for Austenitic Stainless Steel in Air," in Predictive Capabilities in Environmentally Assisted Cracking, ASME publication PVP-99, Dec. 1985.
8. Bamford, W. H., "Fatigue Crack Growth of Stainless Steel Piping in a Pressurized Water Reactor Environment," Trans ASME, Journal of Pressure Vessel technology, Feb. 1979.
9. Roarty, D. H., et al, "Technical Justification for Eliminating Large Primary Loop Pipe Rupture as the Structural Design Basis for Beaver Valley Unit 1," Westinghouse Electric Corp., WCAP 11317, March 1987.

**TABLE 1
PIPING DESIGN LOADS**

	F_x (kips)	M_y (in.-kips)	M_z (in.-kips)
Normal/Upset			
Thermal	-16.5	-1080.9	-992.4
OBE	34.7	2141.3	1200.0
Emergency/Faulted			
DBE	62.82	3011.59	194.13
Surge Unbk LOCA	311.75	116.35	96.10
Accum Unbk LOCA	422.18	65.38	336.43
RHR Unbk LOCA	274.93	116.01	91.61
Surge Broken Loop LOCA	329.24	950.10	75.31
Accum Broken Loop LOCA*	611.08	681.65	18033.89
RHR Broken Loop LOCA	283.58	692.14	131.77
Broken loop, RPV Mot	13.96	569.36	3873.50
Unbk 1 RPV Mot	11.93	274.78	3692.92
Unbk 2 Mot	7.83	748.91	1750.02

TABLE 2
SUMMARY OF PRIMARY SYSTEM TRANSIENTS - BEAVER VALLEY UNIT 1

Number	Transient Identification	Cycles
1	Partial loss of flow	80
2	Inadvertent S.I. Actuation	60
3	Heatup	200
4	Cooldown	200
5	Unit loading at 5% per minute	18300
6	Unit unloading at 5% per minute	18300
7	10% step load increase	2000
8	10% step load decrease	2000
9	Large step load decrease with steam dump	200
10	Feedwater cycling at hot shutdown	2000
11	Loop out-of-service, normal loop startup	70
12	Loop out-of-service, normal loop shutdown	80
13	Reactor trip from full power -- no cooldown	230
14	Reactor trip from full power -- cooldown, no S.I.	160
15	Reactor trip from full power -- cooldown and S.I.	10
16	Inadvertent startup of an inactive loop -- inactive loop	10
17	Inadvertent startup of an inactive loop -- active loop	10
18	Turbine roll test -- heat up	20
19	Turbine roll test -- cooldown	20
20	Loss of load	80
21	Control rod drop	80
22	Loss of power	40
23	Inadvertent RCS depressurization	20
24	Steady state fluctuation	150000

TABLE 3
FATIGUE CRACK GROWTH FOR SURFACE FLAWS - STAINLESS STEEL
CIRCUMFERENTIAL FLAWS

	Initial Crack Depth (inches)	Crack Depth After Year			
		10	20	30	40
Continuous Flaw	0.90	0.9113	0.9232	0.9346	0.9465
	1.0	1.012	1.025	1.037	1.050
	1.07	1.083	1.087	1.110	1.124
Aspect Ratio 40:1	0.90	0.911	0.922	0.933	0.945
	1.0	1.011	1.023	1.034	1.046
	1.15	1.163	1.176	1.188	1.202
Aspect Ratio 20:1	1.20	1.21	1.22	1.231	1.241
	1.40	1.412	1.425	1.438	1.451
	1.50	1.514	1.529	1.543	1.558
Aspect Ratio 10:1	1.20	1.21	1.21	1.22	1.222
	1.40	1.41	1.41	1.42	1.423
	1.50	1.51	1.512	1.519	1.525

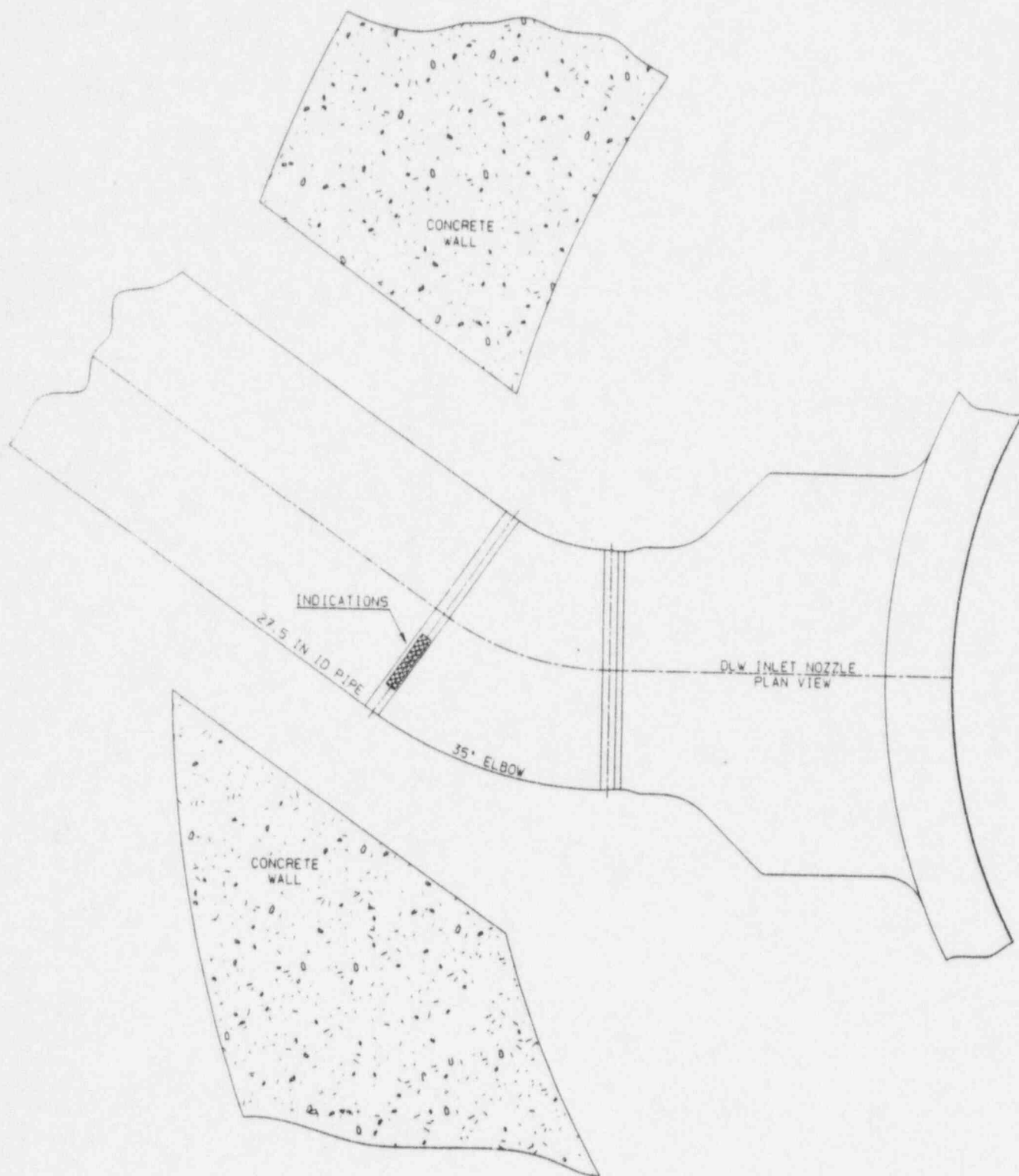


Figure 1 - Geometry and Location of the Indication

LEGEND

A - The 10, 20, 30 year acceptable flaw limits.

B - Within this zone, the surface flaw is acceptable by ASME Code analytical criteria in IWB-3600

C - ASME Code allowable - per Table IWB 3514-2.

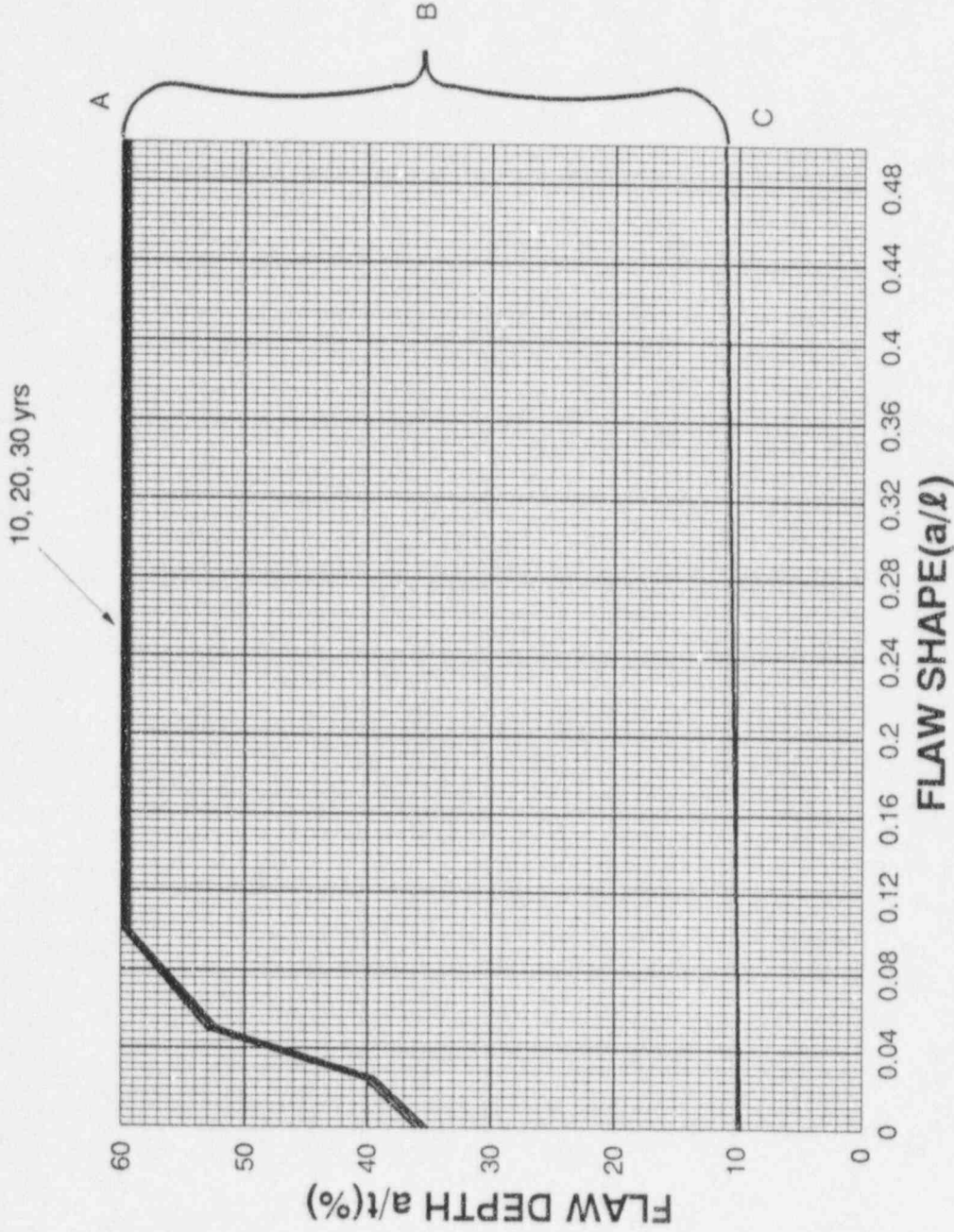


Figure 2 - Flaw Evaluation Chart for the Beaver Valley Unit 1 40 Degree Elbow to Pipe Weld Region: Circumferential Surface Flaws

bvc:37 d/w